Effects of Crystallinity and Molecular Weight on Crack Behavior in Crystalline Poly(L-lactic acid)

Siti Nurkhamidah, Eamor M. Woo

Department of Chemical Engineering, National Cheng Kung University, Tainan 701, Taiwan

Received 7 October 2010; accepted 27 December 2010
DOI 10.1002/app.34021
Published online 13 June 2011 in Wiley Online Library (wileyonlinelibrary.com).

ABSTRACT: The crack behavior and spherulitic morphology in melt-crystallized poly(L-lactic acid) (PLLA) were found to be molecular weight (MW) and crystallinity dependent, along with other key factors. With increasing MW in PLLA, the size of spherulites, band spacing of ring-banded spherulites, and degree of crystallinity decreased, whereas cracks were increasingly less likely to occur. Multiple types of cracks, that is, circumferential and/or radial cracks, were massively present in low-MW PLLA (PLLA-11k), which had a high crystallinity. Upon cooling, in PLLA-11k at most crystallization temperatures (T_c's), cracks formed, and the crack patterns were dependent on the lamellar morphology within the spherulites. Hexagonal, rather than circular, cracks occurred spontaneously during the cooling process of PLLA of a medium-MW grade (PLLA-120k) in PLLA film samples crystallized only at high T_c (135–138°C) and cooled to ambient temperature. However, no cracks of any types at all were present in PLLA films of high enough MWs (PLLA-152k and PLLA-258k) upon either slow air cooling or quench cooling when the samples were dipped into liquid nitrogen. Apparently, cooling-induced contraction differences in different directions were invalid or not sufficient to address the complex cracking behavior in PLLA. In addition, for PLLA-11k with a substantially high crystallinity, cracks were so prone to occur that even cover constraint imposed another factor in determining the crack and ring-band patterns. More plausible mechanisms and correlations between the cracks, MW, crystallinity, spherulite size, and spherulite lamellar patterns of PLLA were analyzed in detail and proposed in this study.
 J Appl Polym Sci 122: 1976–1985, 2011

Key words: crystallization; morphology; polyesters, spherulites; thin films

INTRODUCTION

Poly(L-lactic acid) (PLLA) is a biodegradable and biocompatible polymer that can be used for various biomedical fields.[1–3] PLLA has been reported to be brittle at room temperature and has poor processing properties. The brittleness of materials can be caused by the presence of spherulites via the formation of cracks.[4] Crack formation in the spherulites of a polymer is sometimes observed during crystallization and the cooling process and by contact with solvent.[5–7] Circumferential cracks show up in ringless spherulites of PLLA during the cooling process and on the constrained sample crystallized between two glass slides only, where the band spacing of cracks decreases with increases in the spherulite radius.[8] However, He et al.[9] observed not only circumferential but also hexagonal cracks in ringless spherulites of PLLA melt-crystallized at 135°C after quenching in liquid nitrogen. Rhythmic growth and thermal shrinkage were identified as the two main factors accounting for the formation of those periodic cracks. Concentric cracks formed in the ring-banded and ringless spherulites of poly(trimethylene terephthalate) after they were dipped into chloroform.[10] Recently, PLLA with a low molecular weight (MW) grade has been reported with crack patterns that are influenced by the morphology of spherulites and that occur upon cooling.[11] Ringless spherulites only have circumferential cracks; whereas, ring-banded spherulites not only have circumferential cracks but also radial cracks. Cracks and ring-banded spherulites are interrelated, and circumferential cracks coincide with the dark bands; however, radial cracks coincide with the bright bands in spherulites.

Although cracks in polymers have been preliminarily characterized by some earlier investigators, a common cause has been attributed to contraction differences between the circumferential and radial thermal expansion coefficients.[5,6] However, actual cracks and their formation and patterns can be influenced by many factors beyond simple interpretation of the thermal expansion coefficients' difference in two directions. The MW can be an important factor affecting the crystallization

Correspondence to: E. M. Woo (emwoo@mail.ncku.edu.tw).

Contract grant sponsor: Taiwan's National Science Council (for three consecutive years); contract grant number: NSC 96-2221-E-006-099-MY3.

TABLE I
Basic Physical Properties of PLLAs with Different MWs Used in This Study

Acronym	Supplier	MW (g/mol)	Polydispersity index	Glass-transition temperature (°C)	Melting temperature (°C)
PLLA-11k	Polyscience	11,000	1.8	45.3	155
PLLA-120k	Nature Works (6201D, [L] = 98.5%)	119,400	1.4	58.8	165.3
PLLA-152k	Fluka	152,000	1.5	59	176
PLLA-258k	Aldrich	258,000	2.5	44.3	177

[L] = percentage of L-lactate units.

behavior of polymers. In addition, the crystallization characteristics of PLLA of different MWs were studied by Miyata and Masuko,[12] and they observed that the growth rates of spherulites increased with decreasing MW. This indicated that crystal growth could be inversely proportional to the MWs. However, the PLLA crack behavior in association with MW, crystallinity, and so on, has not been investigated in detail. The behavior of cracks and ring bands and their patterns in PLLA may also be influenced by MW, among other processing parameters. The mechanisms of cracks in PLLA upon crystallization and cooling could be further clarified by understanding the effects of MW, crystal growth, crystallinity, and so on in PLLA, which constitute the aims of this study.

EXPERIMENTAL

Materials and preparation

The PLLAs used in this study were of four different MWs and ranged from a low of 11,000 to a high of 258,000 g/mol (weight-average MWs). These PLLAs were code-named PLLA-11k (Polyscience, Warrington, Pennsylvania) to PLLA-258k (Aldrich, Buchs, Switzerland), where k indicates the values of the MWs of PLLA in the thousands. Table I shows the suppliers and basic physical properties of the PLLA materials used in this study. Samples of PLLAs were prepared by solution-casting with chloroform as the solvent with a concentration of 4 wt % polymer in the solvent. A drop of solution of the polymer was deposited and uniformly spread on a microglass slide at 45°C, and the solvent was allowed to fully evaporate in the atmosphere. A selected sets of film samples of PLLAs on the microglass slide were crystallized in conditions of with or without a top-cover constraint (microglass slide) to compare the results. Samples were heated on a hot stage to a specific maximum melting temperature (T_{max} = 190°C) for 2 min to erase prior crystals and then rapidly removed to another hot stage preset at a designated isothermal crystallization temperature (T_c) ranging from 100 to 140°C.

Apparatus and procedures

For characterization of the morphology in the cast films of PLLA, several microscopic techniques were used. A polarized optical microscope (Nikon Optiphot-2, Tokyo, Japan), equipped with a digital camera charge-coupled device and a microscopic hot stage (Linkam THMS-600, Surrey, UK) with a TP-92 temperature programmer was used to characterize the optical homogeneity and/or crystalline morphology of the blends.

Atomic force microscopy (AFM; Caliber, Veeco-DI Corp., Santa Barbara, CA) investigations were made in intermittent tapping mode with a silicon tip (frequency (f_o) = 70 kHz, radius (r) = 10 nm) installed. The largest scan range was 150 × 150 μm^2, and the scan was kept at 0.5 Hz for the overview scan and zoom regions (5 × 5 μm^2). Thin films were deposited on substrates of glass slides, with an open face for AFM characterization. AFM measurements were also carried out to determine the width and depth of the cracks.

The thermal behavior of the PLLAs was measured with a differential scanning calorimeter (DSC-7, PerkinElmer Corp., Massachusetts, USA) equipped with an intracooler (to −60°C). During thermal annealing or scanning, a continuous nitrogen flow in the differential scanning calorimetry (DSC) sample cell was maintained to ensure minimal sample degradation. Samples were treated in a DSC cell for the intended thermal histories. For melt-crystallization treatments, samples were first melted at 190°C for 2 min and cooled at a rate of 320°C/min to a desired T_c. A heating rate of 10°C/min was used to determine the enthalpy of the melting peak.

RESULTS AND DISCUSSION

Figure 1 shows a diagram summarizing the temperature range of ring-banded versus ringless spherulite morphology for PLLA of different MWs that were crystallized at various T_c's. The spherulite morphology of PLLA melt-crystallized films apparently was affected by the MW, T_c, and presence or absence of a cover constraint. Four grades of PLLA were used

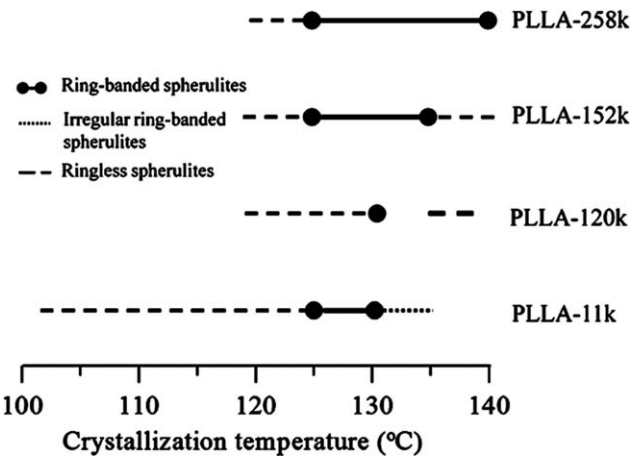

Figure 1 Spherulitic crystalline morphology diagram of PLLA of different MWs as functions of T_c.

in this study. For the low-MW grade (PLLA-11k), ring-banded spherulites only formed at T_c's ranging from 125 to 130°C when crystallization occurred with a top cover. At T_c values lower than 125°C, the morphology was of a pattern of ringless spherulites, but irregular ring-banded spherulites were observed at higher T_c's ($T_c > 130$°C). Uncovered and unconstrained PLLA-11k samples produced no ring bands at all. At $T_c < 125$°C, PLLA-11k formed ringless spherulites crystallized either with or without a top cover. However, dendritic spherulites were observed when PLLA-11k was crystallized at 130–135°C without a top cover.

By comparisons, PLLA-120k (Nature Works, Nebraska, USA), a medium-MW grade PLLA, only showed ring-banded spherulites at 130°C, but the ringless spherulites were observed in PLLA-120k crystallized at T_c's ranging from 120–125 and 135–138°C. For the high-MW grades of PLLAs (PLLA-152k (Fluka, Buchs, Switzerland) and PLLA-258k), the T_c range for ring-banded spherulites was wider than that for the low- and medium-MW grades of PLLA. Ring-banded spherulites were observed at T_c's ranging from 125–135 and 125–140°C in PLLA-152k and PLLA-258k, respectively. In medium- and high-MW PLLA grades, ring-banded spherulites formed from melt-crystallized PLLA either with or without a top cover, which was different for low-MW PLLA. Apparently, ring-banded spherulites of high-MW PLLA formed more easily than those of the low-MW one.

In the ringless or ring-banded spherulites of PLLAs, cracks formed, but they varied with respect to T_c and corresponding lamellar patterns in the spherulites. Figure 2 shows a diagram summarizing the temperature range of cracks in PLLAs of different MWs that were crystallized at various T_c's. For PLLA-11k, cracks occurred spontaneously upon cooling from T_c to ambient temperature at all T_c's (100–135°C). With increasing MW in PLLA, it was apparent that the crack behavior was different, and cracks in PLLAs of high MW were not so readily formed as PLLA-11k. For PLLA-120k, cracks occurred simultaneously upon cooling only at high T_c's (135–138°C). When PLLA-120k was crystallized at a temperature of 130°C (ring-banded spherulites), cracks occurred very slowly in samples held at this T_c (130°C) for several hours (9 h). However, cracks did not form at all when PLLA-120k was crystallized at T_c below 130°C, even though the samples had been cooled to and kept at ambient temperature for up to several days. By contrast, there were no cracks at all T_c's for PLLAs of higher MWs, such as PLLA-152k and PLLA-258k. Only a few sporadic inter-spherulitic cracks appeared during crystallization and cooling in these high-MW PLLAs. Obviously, cracks were more prone to form in low-MW PLLA than in high-MW PLLAs. Interestingly, the trend of crack behavior was opposite with the formation of ring-banded spherulites, as the ring-band spherulites formed more easily in high-MW PLLAs than in low-MW ones.

Figure 3 shows the crack patterns in ring-banded spherulites of PLLA melt-crystallized at $T_c = 130$°C with a top cover. Interestingly, with increasing MW, the size of the spherulites and band spacing of the ring-banded spherulites decreased. The crack patterns were also different when the MW of PLLA was different. For low-MW PLLAs (PLLA-11k), there were numerous types of cracks: (1) tiny tribranched cracks near the center of the spherulites, (2) twin-circumferential cracks coinciding with the dark bands in the spherulites, and (3) radial short-segmental voids coinciding with the bright bands in spherulites, as shown in Figure 3(e). For PLLA-11k crystallized at 120°C, the crack pattern was circular and with smooth circumferential cracks; however, the cracks became irregular when the morphology was a pattern

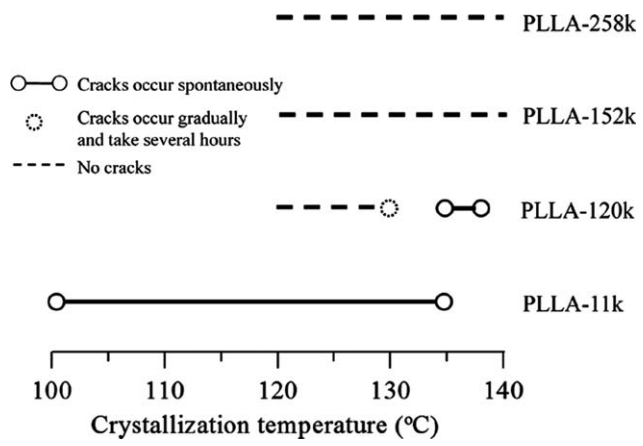

Figure 2 Diagram showing the temperature range of cracks in PLLAs of different MWs as a function of T_c.

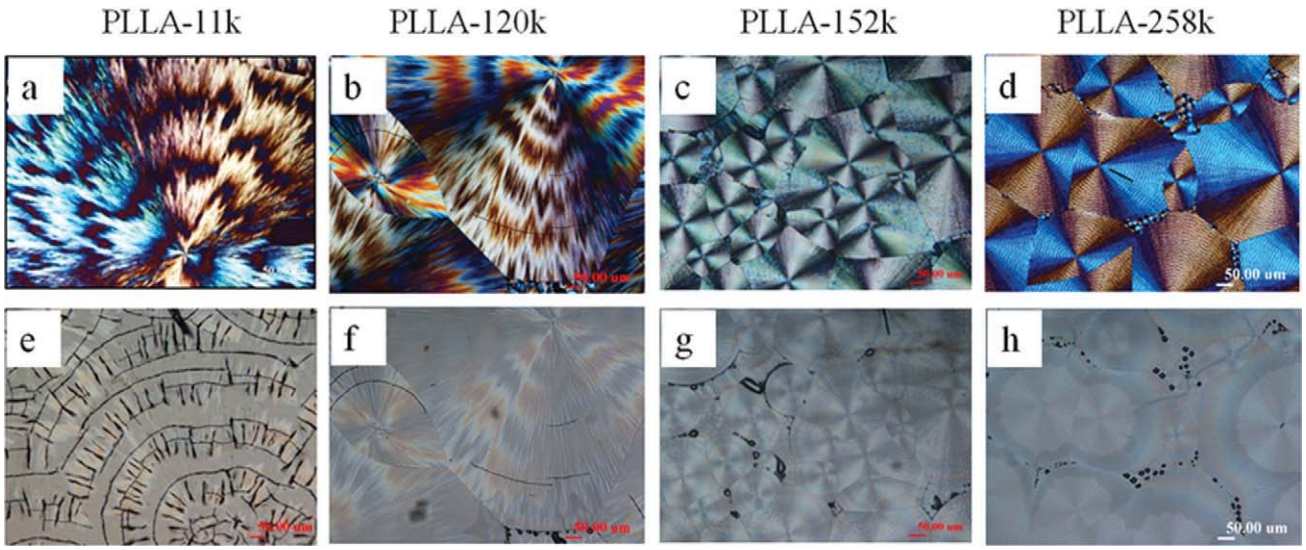

Figure 3 Crack patterns in correlation with ring-banded patterns in PLLA melt-crystallized at $T_c = 130°C$ with the top cover (constrained). [Color figure can be viewed in the online issue, which is available at wileyonlinelibrary.com.]

of dendritic spherulites ($T_c = 130°C$).[11] As discussed earlier, the cracks in PLLA-120k did not occur spontaneously during the cooling process. Figure 3(f) shows the circumferential cracks in PLLA-120k, which occurred during the cooling process, and the graph taken at ambient temperature after the sample was held at this temperature for 9 h. For PLLA-152k and PLLA-258k, only a few interspherulitic cracks occurred during the crystallization process, but no additional cracks of other types occurred during further cooling from T_c to ambient temperature. The interspherulitic cracks shown in Figure 3(g,h) were similar to the cracks in polyhydroxybutyrate, which reportedly were caused by a significant negative pressure due to the volume change on crystallization.[7] The fact that there was considerable stress in the samples caused by the volume reduction on crystallization was evidenced by the appearance of voids/bubbles near the growth front.

Cracks not only occurred in the ring-banded spherulites but also in the ringless spherulites of PLLAs upon cooling from T_c to ambient temperature; however, the crack patterns differed, depending on the lamellar patterns (ringless vs ring-banded) on the spherulites set up at T_c. Among the four MW grades of PLLAs used in this study, only the ringless spherulites of PLLA-11k and PLLA-120k showed cracks during the cooling process, as shown and discussed earlier for Figure 2. The cracks were also examined and compared to the ringless spherulites of PLLAs of various MWs. Figure 4 shows the crack patterns in the ringless spherulites of PLLA-120k melt-crystallized at $T_c = 135°C$ without a top cover. The crack pattern of PLLA-120k crystallized either with or without a top cover at 135°C was of a hexagonal geometry, in which the cracks occurred simultaneously upon cooling. Apparently, for PLLA-120k, the cracks occurred simultaneously when the

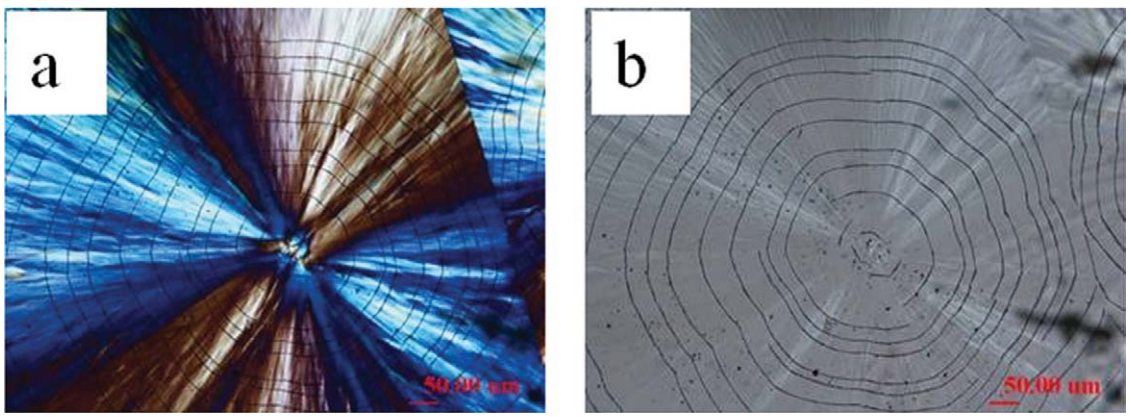

Figure 4 Crack patterns in ringless spherulites of PLLA-120k melt-crystallized at $T_c = 135°C$ without top cover. [Color figure can be viewed in the online issue, which is available at wileyonlinelibrary.com.]

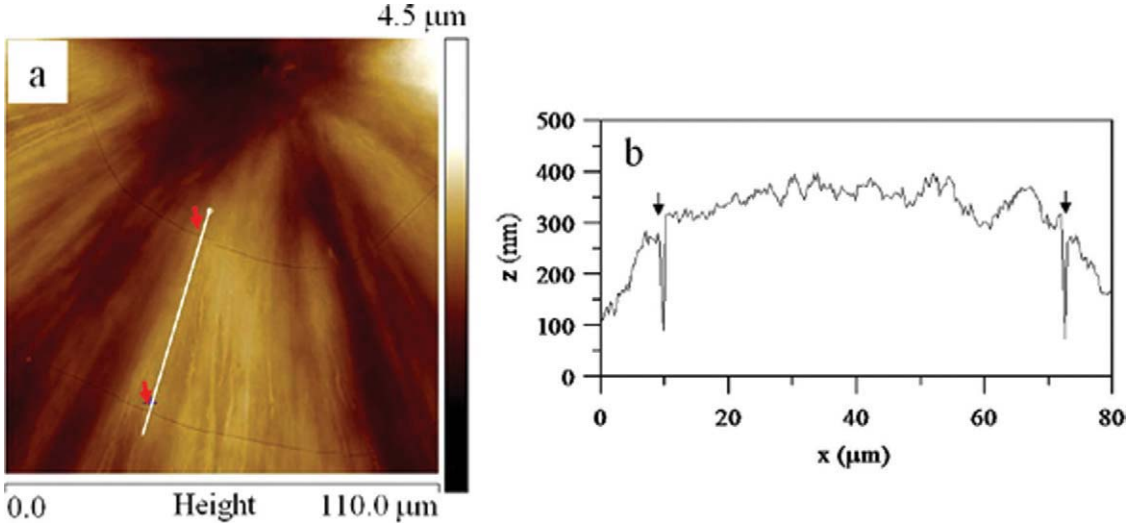

Figure 5 AFM results for PLLA-120k melt-crystallized at $T_c = 135°C$ without the top cover: (a) height image and (b) height profile measured along the white line in part a. [Color figure can be viewed in the online issue, which is available at wileyonlinelibrary.com.]

samples were crystallized at higher T_c's (135–138°C). A similar hexagonal crack pattern in PLLA was reported by He et al.,[9] who suggested that the hexagonal-shaped cracks might have resulted from the (110) growth plane as hexagonal-shaped crystals are formed at the early stage of melt crystallization at 135°C. It must be noted here that cracks of different geometry, such as circular geometry, are also possible for PLLA crystallized at other T_c's.

Figure 5 shows the AFM results for PLLA-120k melt-crystallized at $T_c = 135°C$ without a top cover. Figure 5(a) shows the height image, and Figure 5(b) shows height profile measured along the white line in Figure 5(a). Cracks in the AFM height image and height profile are indicated by arrows. Two neighboring hexagonal cracks can be seen obviously in Figure 5(a), and the average crack depths along the white line were about 200 nm. For PLLA-11k, either crystallized with or without a top cover, the depth of the cracks increased with increasing T_c, with the maximum value at $T_c = 125°C$, and decreased with further increases of T_c.[11] Therefore, the depth of cracks observed in the spherulites could be deeper than what was experimentally measured with AFM. There is possibility that the tip could not scan all areas inside the cracks.

As discussed previously, no cracks appeared in the high-MW PLLAs upon cooling from T_c to ambient temperature. He et al.[9] suggested earlier that thermal shrinkage because of different coefficient of thermal expansion in radial versus circumferential directions is one of the main factors in the formation of cracks. However, it is noted later that the cracks of many different types in PLLAs of

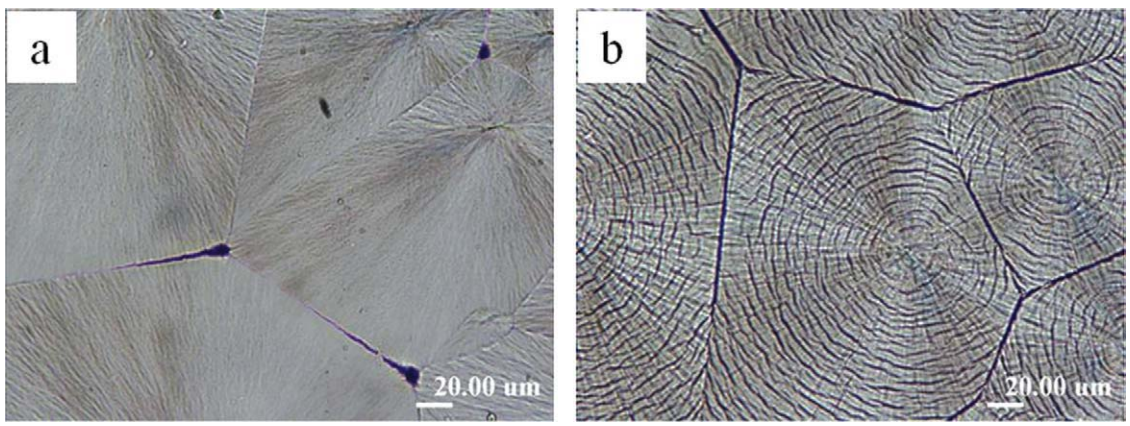

Figure 6 OM micrographs of PLLA-152k melt-crystallized at $T_c = 140°C$ without the top cover (unconstrained). Graphs taken at (a) T_c and (b) ambient temperature after the samples were quenched in liquid nitrogen. [Color figure can be viewed in the online issue, which is available at wileyonlinelibrary.com.]

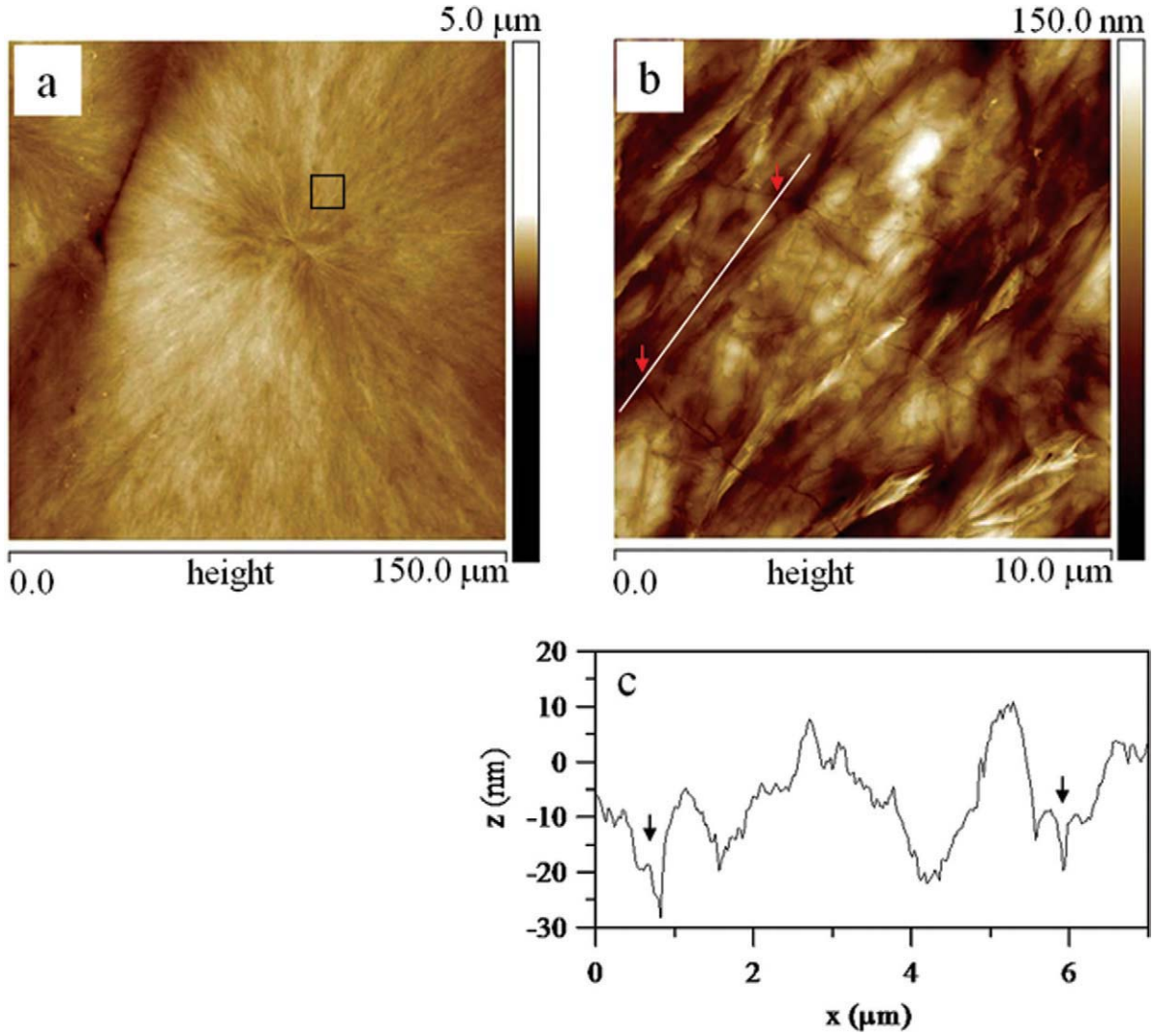

Figure 7 AFM results for PLLA-152k melt-crystallized at T_c = 140°C without the top cover then quenched in liquid nitrogen: (a) AFM height image, (b) AFM height image of magnified square area in part a, and (c) AFM height profile along the white line in part b. [Color figure can be viewed in the online issue, which is available at wileyonlinelibrary.com.]

various MWs in this study could not all be fully interpreted or satisfactorily accounted for by the simple differences of the coefficient of thermal expansion in two directions. Furthermore, the depth profiles of these cracks, as revealed in AFM analyses to be discussed later, may have complicated the situation. Figure 6 shows the optical microscope (OM) micrographs of PLLA-152k melt-crystallized at T_c = 140°C without a top cover. The graphs were taken at T_c [Fig. 6(a)] and ambient temperature [Fig. 6(b)] after the samples were quenched into liquid nitrogen. As shown earlier in Figure 2, there were no cracks in the ringless spherulites of PLLA-152k crystallized at T_c = 140°C upon cooling to ambient temperature. No cracks occurred during the crystallization process at T_c, as shown in Figure 6(a). The crystallized PLLA-152k sample with T_c = 140°C was then dipped into liquid nitrogen and equilibrated at ambient for OM characterization. However, Figure 6(b) shows that only extensive concentric wrinkles, but no cracks, appeared in the ringless spherulites in the fully crystallized PLLA-152k sample quenched into liquid nitrogen. Note, however, the wrinkles were not to be mistaken as cracks. Still, there were no cracks in the liquid-N_2 quenched PLLA-152k samples (having been crystallized at T_c = 140°C).

The depth of these concentric wrinkles in the PLLA-152k samples was also measured with AFM. Figure 7 shows the AFM images of PLLA-152k melt-crystallized at T_c = 140°C without a top cover and then quenched into liquid nitrogen [Fig. 7(a), AFM height image; Fig. 7(b), AFM height image of the black square area in Fig. 7(a); and Fig. 7(c), AFM height profile along the white line marked in Fig.

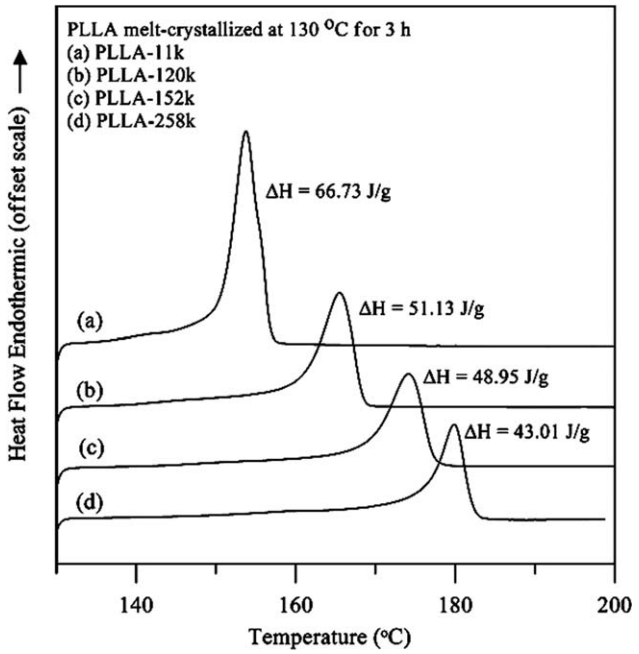

Figure 8 DSC curves showing the crystallinities of PLLAs of different MWs melt-crystallized at 130°C for 3 h.

7(b)]. In contrast with the cracks in PLLA-11k and PLLA-120k, the concentric wrinkles could not be seen in the AFM height image with a big scan area (150×150 μm^2), as shown in Figure 7(a). However, concentric wrinkles could be observed after we zoomed into a scan area of 10×10 μm^2 [black square area in Fig. 7(a)], as indicated by the red arrows in Figure 7(b). Figure 7(c) shows that the height profile along the white line in Figure 7(b) crossed two neighboring concentric wrinkles, and the arrows in this figure corresponded to the arrows in Figure 7(b). Concentric wrinkles could not be seen in a large scan area because the depth of concentric wrinkles was very narrow, only 10 nm in depth.

Apparently, the cracks that occurred upon cooling to ambient temperature in the PLLA-11k and PLLA-120k samples were significantly different from the concentric wrinkles in PLLA-152k after they were quenched into liquid nitrogen. That is, the topology and internal structures of wrinkles in PLLA were not the same as those of the cracks. Additionally, for a fully crystallized sample quenched to −150°C with liquid nitrogen, the thermal shrinkage obviously was much larger than that quenched by cooling of the same sample from T_c to ambient temperature. However, no cracks, only concentric wrinkles appeared in films of high-MW PLLA-152k quenched into liquid nitrogen. This result indicates that the thermal shrinkage was not the only factor and may not have been the main factor influencing the formation of cracks in PLLA. Crystalline characteristics in PLLA and crystal packing patterns constituted some of the main factors accounting for the cracks.

As discussed earlier, cracks were more prone to occur in PLLA-11k, as shown earlier in Figure 2. Also as shown earlier in Figure 3, the crack patterns were different in different MW PLLAs when they were crystallized at the same T_c (130°C). Apparently, the MW in PLLA is highly influential on the tendency to form cracks. As cracks are related to crystals in PLLA, it would be intuitive to suggest that the MWs of PLLA might be related to the crystallinity levels in PLLAs. The crystallinity of all MW grades of PLLA used in this study was measured with DSC to reveal whether the crystallinity might be a factor in the formation of cracks. From the DSC curves shown in Figure 8, the melting endothermic enthalpy (ΔH_m) decreased with increasing MW of PLLA. The crystallinity of PLLA could be calculated with the following equation: $X_c = \Delta H_m / \Delta H_m^o \times 100\%$,[13] where X_c is degree of crystallinity and ΔH_m^o is the melting endothermic enthalpy of perfect crystals. Various values of ΔH_m^o for perfect crystals in PLLA have been reported, ranging from 91 to 148 J/g.[14–18] A value of 91 J/g reported by Wunderlich[15] was used to estimate X_c of the PLLAs used in this study.

The calculated values of X_c in Table II show that the degree of crystallinity proportionally decreased with increasing MW of the PLLAs, which on average ranged from 73.3% for the lowest MW PLLA to 47.3% for the highest MW PLLA. Apparently, the level of MW of PLLA influenced the tendency of crystallization and, thus, its maximum crystallinity. In turn, the crystallinity in PLLA had determining effects on the formation of cracks. Cracks were more prone to occur in the samples with a high crystallinity (or low MW, such as PLLA-11k), but cracks were rare or entirely absent in PLLAs of a low crystallinity (or high MWs, such as PLLA-152k and PLLA-258k). In addition, it is known that fully amorphous poly(D,L-lactic acid) does not form cracks at all when it is heated and then cooled.

To further clarify the effects of MW or crystallinity on the formation or patterns of cracks, blends of PLLA-11k with each of the three different MWs of PLLAs (PLLA-120k, PLLA-152k, and PLLA-258k), respectively, were prepared at a fixed 50/50 composition and characterized to correlate the cracks and spherulite morphology. Figure 9 shows the spherulitic morphology and crack pattern of the high-MW

TABLE II
Crystallinity of PLLAs as Measured by DSC Melting Peak Enthalpy

Material	ΔH_m (J/g)	X_c (%)
PLLA-11k	66.73	73.33
PLLA-120k	51.13	56.19
PLLA-152k	48.95	53.49
PLLA-258k	43.01	47.26

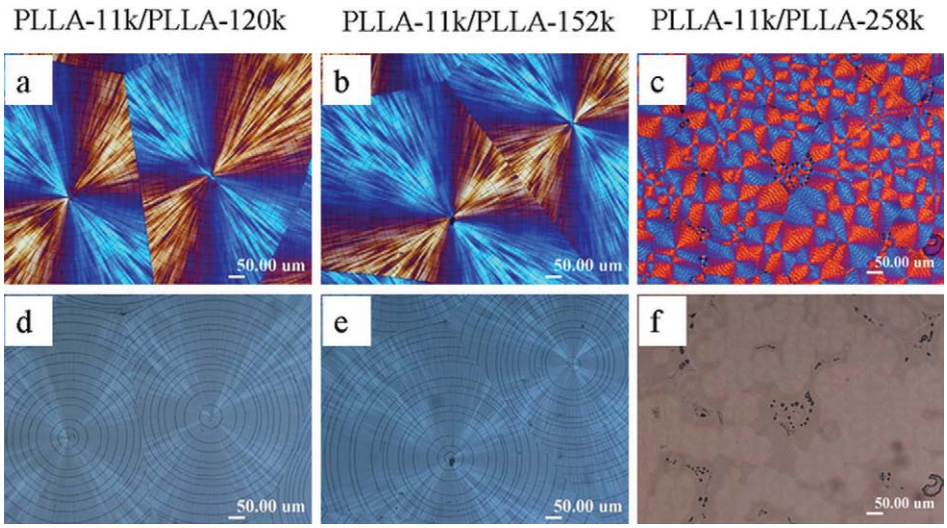

Figure 9 Spherulitic morphology and crack pattern of high-MW PLLA blends with low-MW PLLA (50/50) melt-crystallized at $T_c = 130°C$ with the top cover (constrained). [Color figure can be viewed in the online issue, which is available at wileyonlinelibrary.com.]

PLLA/low-MW PLLA blends (50/50) melt-crystallized at $T_c = 130°C$ with a top cover (constrained). As shown earlier in Figure 3, when crystallized at $T_c = 130°C$, the sample films of PLLAs of various MWs showed ring-banded spherulites in which the band spacing of ring-banded spherulites decreased with increasing MW. However, the morphology of the PLLA blends [(PLLA-11k/PLLA-120k), (PLLA-11k/PLLA-152k), and (PLLA-11k/PLLA-120k)] at $T_c = 130°C$ was that of ringless spherulites. The spherulitic morphology of PLLA-11k/PLLA-120k and PLLA-11k/PLLA-152k blends was similar, showing ringless spherulites with smooth surface. Both blends exhibited concentric cracks during the cooling process from T_c to ambient temperature. In contrast, the PLLA-11k/PLLA-258k blend did not show any cracks during cooling,

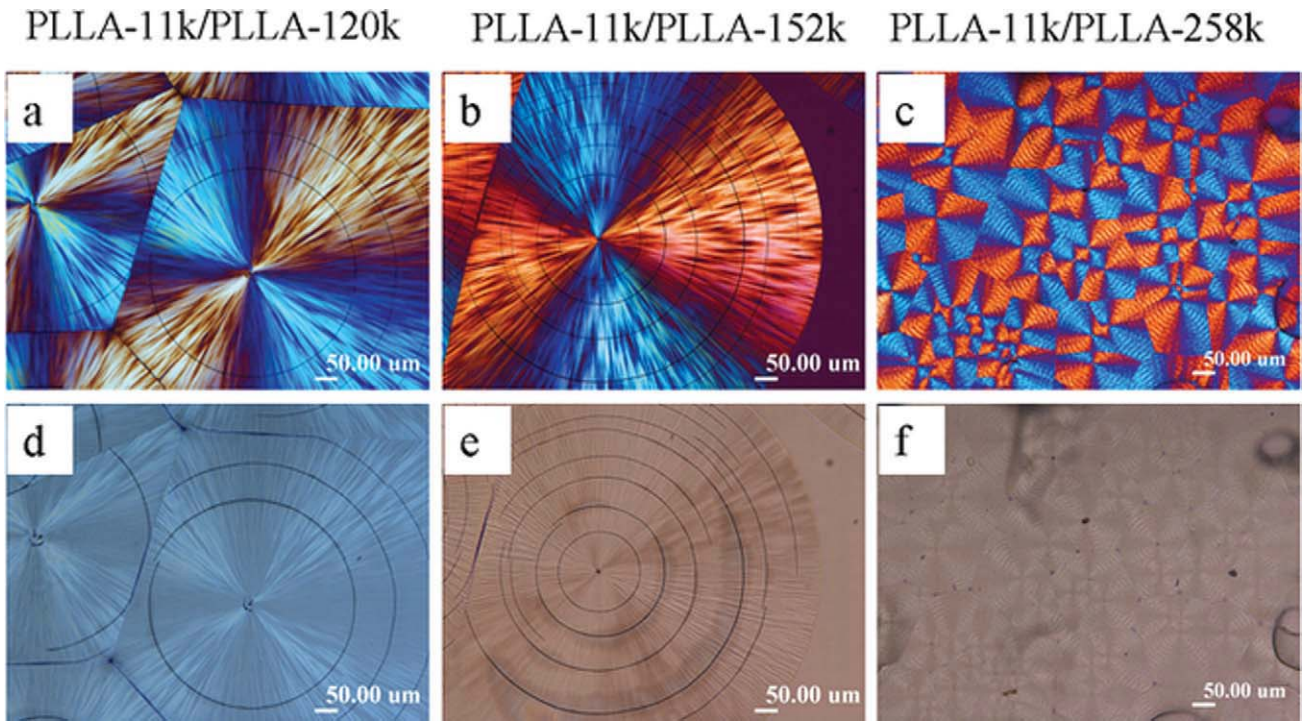

Figure 10 Spherulitic morphology and crack pattern of the high-MW PLLA blends with low-MW PLLA (50/50) melt-crystallized at $T_c = 130°C$ without the top cover (unconstrained). [Color figure can be viewed in the online issue, which is available at wileyonlinelibrary.com.]

even after they were kept at ambient temperature for several hours. There were no cracks in the PLLA-11k/PLLA-258k blend; this may have been due to fact that the lamellar pattern in the ringless spherulites of the blend was more dense or compact than that of the other PLLA blends.

Figure 10 shows polarized optical microscopy graphs for spherulitic morphology and crack patterns of high-MW PLLA (120k, 152k, and 258k) blends with low-MW PLLA (50/50) melt-crystallized at $T_c = 130°C$ without a top cover (unconstrained). In general, blends of low-MW PLLA with higher MW PLLA (e.g., 258k) showed much fewer or almost no cracks within the spherulites. In addition, a comparison with the polarized optical microscopy results for the covered samples, shown earlier in Figure 9, revealed that the intercrack spacing of the cracks differed, depending on whether the samples were covered or not. However, the crack patterns and spherulite morphology did not seem to change much with or without a cover. The difference was only in the spacing of cracks. Without a top cover, the spacing of the cracks was larger than that with a top cover. However, the crystalline ring-banded morphology remained the same with or without a cover. With the top cover (two constraints), the intercrack spacing in the crystallized spherulites was narrower. By comparison, higher MW grades of PLLAs exhibited much fewer cracks or almost no cracks upon crystallization, either with or without top covers. Note, however, that the thermal shrinkages were almost the same for low- or high-MW PLLAs; but higher MW grades of PLLAs showed progressively fewer cracks. Thermal shrinkage alone may not have fully accounted for the cracks. In addition to the factor of thermal shrinkage, the PLLAs with a high MW had a lower crystallinity and lower rates of crystal growth, which influenced the extent of cracking. A top cover on the PLLA samples further complicated the issue by exerting additional constraints. Note that the film thickness between the two constraints may have imposed another factor on cracking. The effect of films thickness was beyond the scope of this study, and thus, it is not discussed here. Therefore, it was hard to attribute the crack patterns to thermal shrinkage only. The even constraints exerted by the two covers on the samples most likely were responsible for the more closely spaced cracks than those in the samples with the single constraint only from the bottom substrate (with the sample top open to air).

Figure 11 shows the DSC curves of the PLLA blends (50/50) melt crystallized at 130°C for 3 h. As shown earlier in Figure 8, the neat PLLA-11k and PLLA-120k had an endothermic enthalpy (crystal melting) higher than 50 J/g, and they did exhibit cracks. However, the ΔH_m of PLLA-152k and PLLA-258k was less than 50 J/g, and there were no cracks appearing during the cooling process. By comparison, they were blended with PLLA-11k, ΔH_m of PLLA-120k, PLLA-152k, and PLLA-258k increased to values higher than 50 J/g. Only when PLLA-11k was blended with high-MW PLLA (PLLA-258k) did the high-MW PLLA/low-MW PLLA blend not show any cracks, even though the endothermic enthalpy of crystal melting was high. These results summarily show that the MW, crystallinity, and ringless or ring-banded lamellar patterns in the spherulites of the PLLAs were intricately correlated with the crack tendency and patterns. Apparently, cooling-induced contraction differences in different directions were invalid or were not sufficient to address the complex cracking behavior in PLLA. More plausible mechanisms should take into full account the correlations between the cracks, MW, crystallinity, spherulite size, and lamellar patterns in spherulites of PLLA, as discussed previously.

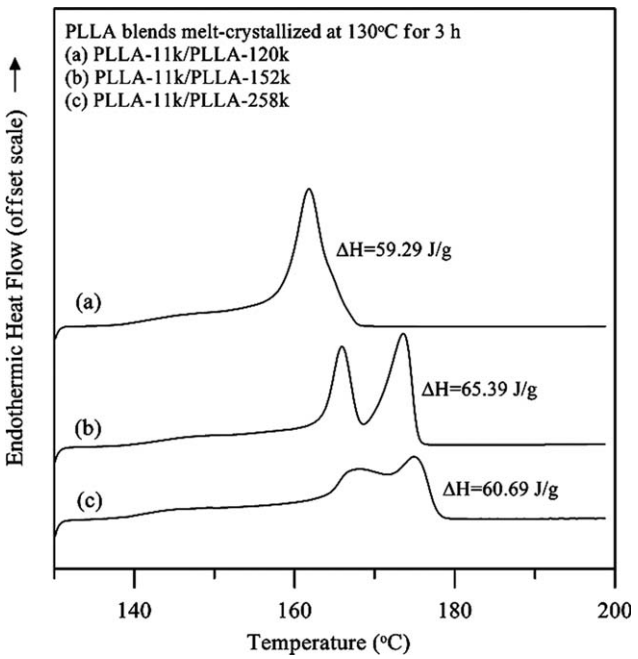

Figure 11 DSC curves showing crystallinities of the high-MW PLLA blends with low-MW PLLA (50/50) melt-crystallized at 130°C for 3 h.

CONCLUSIONS

The extents of cracks and general crack behavior in spherulites of PLLA of various MWs apparently were affected by the MW and crystallinity, among other factors, of the PLLA. The lamellar patterns, in association with ringless or ring-banded spherulites and spherulite sizes, also influenced the crack shapes, depths, and severity. The spherulite size and ring-band spacing of PLLA decreased with increasing MWs. Ring-banded spherulites were more easily formed in high-MW grades (PLLA-152k and PLLA-258k) with a wider range of T_c's when crystallized

with or without a cover constraint. Cracks were more prone to occur in low-MW grades (PLLA-11k), and the cracks of up to three types occurred immediately during cooling from all crystallization processes (100–135°C) to ambient temperature. For the medium-MW grade of PLLA (PLLA-120k), the cracks occurred only during cooling from higher T_c (135–138°C) to ambient temperature, but no cracks were seen upon cooling from lower T_c (e.g., 120°C or lower) to ambient temperature.

By contrast, there were no cracks in the crystallized samples of high-MW PLLAs (PLLA-152k or PLLA-258k) upon either slow air cooling or quench cooling by the dipping of the samples into liquid nitrogen whose higher MWs tended to have lower crystallinities. No intraspherulitic cracks were present, and only occasional interspherulitic cracks (cracks along the interfaces between two neighboring spherulites and not within a spherulite) were present because of the overall volume reduction on crystallization and cooling. Apparently, the earlier proposed mechanism of cooling-induced contraction differences in radial versus circumferential directions might have been invalid or not sufficient to address the complex cracking behavior in PLLA showing various types of cracks beyond such a simple interpretation. The crack patterns in the PLLAs were dependent on the lamellar morphology within the spherulites set up at T_c; further cooling initiated cracks along the interfaces of the lamellae of different orientations and/or crystalline lamellae–amorphous boundaries. More plausible mechanisms and correlations between the cracks, MWs, crystallinity, spherulite size, and spherulite lamellar patterns of PLLA were fully expounded in this study.

References

1. Penning, J. P.; Dijkstra, H.; Pennings, A. J. Polymer 1993, 34, 942.
2. Albertsson, A. C.; Varma, I. K. Biomacromolecules 2003, 4, 1466.
3. Kim, H. D.; Bae, E. H.; Kwon, I. C.; Pal, R. R.; Nam, J. D.; Lee, D. S. Biomaterials 2004, 25, 2319.
4. Burns, S. J. Scr Mater 1996, 35, 925.
5. Barham, P. J.; Keller, A. J. J Polym Sci Part B: Polym Phys 1986, 24, 69.
6. Martinez-Salazar, J.; Sanchez-Cuesta, M.; Barham, P. J.; Keller, A. J Mater Sci Lett 1989, 8, 490.
7. Hobbs, J. K.; McMaster, T. J.; Miles, M. J.; Barham, P. J. Polymer 1996, 37, 3241.
8. Fraschini, C.; Plesu, R.; Sarasua, J. R.; Prud'homme, R. E. J Polym Sci Part B: Polym Phys 2005, 43, 3308.
9. He, Y.; Fan, Z.; Wei, J.; Li, S. J. Polym Eng Sci 2006, 46, 1583.
10. Kuboyama, K.; Ougizawa, T. Polym J 2008, 40, 1005.
11. Nurkhamidah, S. M.S. Thesis, National Cheng Kung University, Tainan, Taiwan, 2009.
12. Miyata, T.; Masuko, T. Polymer 1998, 39, 5515.
13. Pan, P.; Liang, Z.; Nakamura, N.; Miyagawa, T.; Inoue, Y. Macromol Biosci 2009, 9, 585.
14. Fisher, E. W.; Sterzel, H. J.; Wegner, G. Kolloid Z Z Polym 1973, 251, 980.
15. Pyda, M.; Bopp, R. C.; Wunderlich, B. J Chem Therm 2004, 36, 731.
16. Cohn, D.; Younes, H.; Marom, G. Polymer 1987, 28, 2018.
17. Gilding, D. K.; Reed, A. M. Polymer 1979, 20, 1459.
18. Loomis, G. L.; Murdoch, J. R. Polym Prepr 1990, 31, 55.